Influence of the anisotropy on zero-group velocity Lamb modes

Claire Prada[a] and Dominique Clorennec
Laboratoire Ondes et Acoustique, ESPCI-Université Paris 7-CNRS, UMR 7587, 10 rue Vauquelin, 75231 Paris Cedex 05, France

Todd W. Murray
Department of Mechanical Engineering, Boston University, 110 Cummington Street, Boston, Massachusetts 02215

Daniel Royer
Laboratoire Ondes et Acoustique, ESPCI-Université Paris 7-CNRS, UMR 7587, 10 rue Vauquelin, 75231 Paris Cedex 05, France

(Received 19 March 2009; revised 9 June 2009; accepted 11 June 2009)

Guided waves in a free isotropic plate (symmetric S_n and antisymmetric A_n Lamb modes) exhibit a resonant behavior at frequencies where their group velocity vanishes while their phase velocity remains finite. Previous studies of this phenomenon were limited to isotropic materials. In this paper, the optical generation and detection of these zero-group velocity (ZGV) Lamb modes in an anisotropic plate is investigated. With a circular laser source, multiple local resonances were observed on a silicon wafer. Experiments performed with a line source demonstrated that the frequency and the amplitude of these resonances depend on the line orientation. A comparison between experimental and theoretical dispersion curves for waves propagating along the [100] and [110] directions of the silicon crystal verified that these resonances occur at the minimum frequency of the S_1 and A_2 Lamb modes. Simulations indicated that it is possible to deduce the three elastic constants of the plate material with good accuracy from these measurements.
 [DOI: 10.1121/1.3167277]

PACS number(s): 43.40.Dx, 43.35.Yb, 43.20.Mv [YHB] Pages: 620–625

I. INTRODUCTION

Lamb waves are frequently used in the ultrasonic characterization of thin plates. Most approaches proposed in the literature use the dispersion characteristics of these waves to extract the mechanical properties or thickness of a given plate. Laser-based ultrasonic techniques are particularly attractive for exciting and detecting Lamb waves due to the fact that remote measurements can be made without the need for a coupling media.[1,2] In the simplest case, a pulsed laser source focused to a point or a line is used to excite broad band Lamb waves that are detected after a given propagation distance using an optical interferometer.[3–6] Lamb waves of a given wavelength can be excited by the interference of two laser sources, creating a sinusoidal intensity pattern on the sample surface.[7,8] The laser source may also be scanned over the sample surface to preferentially launch Lamb waves with a phase velocity matching the velocity of the moving source.[9] In both cases, the phase velocity is measured as a function of frequency to extract material property information, and a moderate propagation distance is required to measure the velocities with sufficient accuracy.

Recently, a new approach that allows for local measurements of the elastic properties or thickness of various plates was demonstrated. It is based on the excitation by a laser source of a sharp resonance at the minimum frequency of the first symmetric S_1 Lamb mode, where the group velocity of the mode goes to zero while the phase velocity remains finite. The laser source can be either an amplitude-modulated laser that generates Lamb waves at a particular frequency[10] or a pulsed laser that excites the resonant response in the time domain.[11] The plate vibration can then be measured at the excitation point on the sample surface using an optical interferometer. The remarkably high quality factor at megahertz frequencies of these zero group velocity (ZGV) resonances can be used for mapping nanometer scale thickness variations in thin plates as well as for the local measurement of material properties.[12] In addition to laser-based excitation, Holland and Chimenti[13] observed a strong transmission of air-coupled ultrasound at the S_1 ZGV resonance frequency in millimeter thick plates. Gibson and Popovics[14] also demonstrated that resonance observed in concrete during impact-echo testing corresponds to the S_1 ZGV Lamb mode.

Previous experimental studies of the S_1 ZGV resonance phenomena have been limited to isotropic materials. In this paper, the authors extend this analysis to anisotropic materials and study the local, transient response of a thin silicon plate to pulsed laser heating. Anisotropic plates, often comprised of either single crystal or composite materials, are employed for a multitude of applications in, for example, the aerospace, defense, microelectronic, and medical device industries.[15] The ZGV resonance differs markedly in anisotropic media in that the ZGV resonance frequency itself shows directional dependence. The excitation laser source shape can be selected to excite a band of resonance frequen-

[a]Author to whom correspondence should be addressed. Electronic mail: claire.prada-julia@espci.fr.

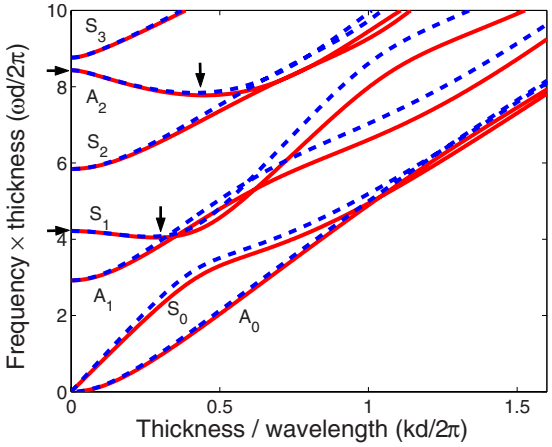

FIG. 1. (Color online) Dispersion curves in the (ω,k)-plane for Lamb waves propagating in a silicon plate of thickness d along the [100] axis (solid lines) and the [110] axis (dashed lines). Vertical arrows correspond to ZGV modes, and horizontal ones to thickness resonance frequencies.

cies over all propagation angles in the sample or to excite a narrow ZGV resonance in a given direction. A laser line source, for example, can be used to generate a sharp ZGV resonance in the direction perpendicular to the line. In this case, the ZGV resonance frequency can be "tuned" by rotating the excitation laser line source with respect to the sample. Laser generated ZGV resonance can be utilized for the local and noncontact nondestructive characterization of anisotropic plates.

II. ZGV LAMB MODES

The propagation of Lamb waves (frequency f, wavelength λ) is represented by a set of dispersion curves in the angular frequency $(\omega=2\pi f)$ and the wave number $(k=2\pi/\lambda)$ plane.[16] It is judicious to use variables normalized to the plate thickness d, such as the frequency thickness product $fd=\omega d/2\pi$ and the thickness to wavelength ratio $d/\lambda=kd/2\pi$. A silicon crystal of cubic symmetry is characterized by three elastic constants: $c_{11}=165.6$ GPa, $c_{12}=63.9$ GPa, $c_{44}=79.5$ GPa, and a mass density $\rho=2329$ kg/m^3. Figure 1 shows, for a [001]-cut silicon plate, the dispersion curves of the lower order symmetric and antisymmetric modes calculated with the software DISPERSE.[17] Curves were calculated for propagation directions along the [100] axis (azimuth angle $\varphi=0°$) and the [110] axis ($\varphi=45°$). For other directions, dispersion curves of a given mode lie inside the bundle delimited by these curves. The lowest order symmetric (S_0) and antisymmetric (A_0) modes originate at zero frequency, while all higher modes originate at a cut-off frequency f_c associated with either the longitudinal (V_L) or shear (V_T) wave velocity in the [001]-plate thickness direction:

$$V_L=\sqrt{c_{11}/\rho}=8433 \text{ m/s},$$

$$V_T=\sqrt{c_{44}/\rho}=5843 \text{ m/s}. \quad (1)$$

It can be observed that for high order modes, the group velocity $V_g=d\omega/dk$ vanishes at $k=0$, giving rise to a thickness resonance at the cut-off frequency. In addition, the group velocity of the first symmetric (S_1) and second antisymmetric (A_2) Lamb modes also vanishes for finite values of the wave number and wavelength $(k_0=2\pi/\lambda_0)$. At these ZGV points the acoustic energy, which cannot propagate in the plate, is trapped in the vicinity of the source. For the S_1 ZGV mode: $\lambda_0=3.50d$ and $3.80d$ in the [100] and [110]-directions, respectively. Thus, the vibration at the minimum frequency f_0 is localized in a region of dimension $\lambda_0/2$ approximately equal to twice the plate thickness. While this behavior is similar to that of an isotropic material,[12] an important distinction is that f_0 is dependent on the propagation direction. It has been shown on isotropic plates that the resulting local resonance can be efficiently excited by a laser pulse and optically detected by a sensitive interferometer.[10]

III. EXPERIMENTAL RESULTS

Experiments were carried out on a commercially available silicon wafer of thickness $d=525\pm5$ μm and diameter equal to 125 mm. Lamb waves were generated in the thermoelastic regime by a Q-switched Nd:YAG (yttrium aluminum garnet) laser (optical wavelength $\Lambda=1064$ nm) providing pulses having a 20-ns duration and 4-mJ of energy. The spot diameter of the unfocused beam is equal to 1 mm. Lamb waves were detected by a heterodyne interferometer[18] equipped with a 100-mW frequency doubled Nd:YAG laser (wavelength $\Lambda=532$ nm). This interferometer is sensitive to any phase shift along the path of the optical probe beam reflected by the moving surface. The contribution due to the local vibration of the plate is proportional to the component u of the mechanical displacement in the x-direction normal to the surface:

$$\Delta\phi_u=\frac{4\pi}{\Lambda_0}u. \quad (2)$$

In many experiments the source and detection points are superimposed. The laser energy absorption heats the air in the vicinity of the surface and produces a variation Δn of the index along the optical path of the probe beam $(0<x<L)$. The resulting phase shift:

$$\Delta\phi_n=\frac{4\pi}{\Lambda_0}\int_0^L \Delta n(x)dx \quad (3)$$

induces a very large low frequency voltage, which saturates the electronic detection circuit. This spurious thermal effect is eliminated by interposing a high-pass filter having a cut-off frequency equal to 1 MHz. The calibration factor for mechanical displacement normal to the surface (10 nm/V) was constant over the detection bandwidth (1–20 MHz). Signals detected by the optical probe were fed into a digital sampling oscilloscope and transferred to a computer.

Figure 2(a) shows that the first 50 μs of the acoustic signal exhibit a series of maxima and minima regularly spaced by 3.3 μs, which reveals the existence of frequency beats. The frequency spectrum in Fig. 2(b), obtained from the whole signal (300 μs), is composed of two parts: a spread spectrum in the low-frequency range, corresponding to the non-resonant A_0 mode, and several sharp peaks. Taking into account the minimum frequency of the S_1 and A_2 branches in Fig. 1 and the nominal plate thickness (d

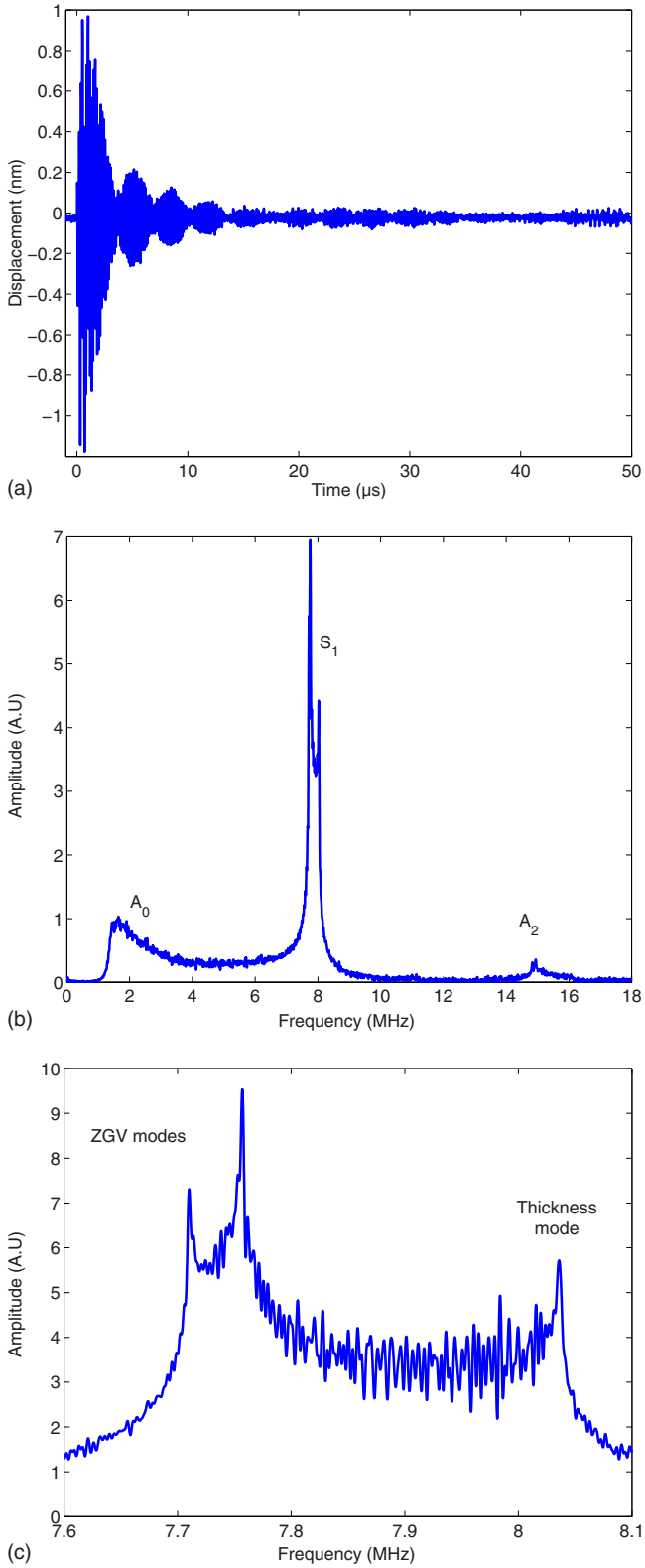

FIG. 2. (Color online) Point laser source. (a) Signal generated by the pulsed laser on a thin silicon plate and detected at the same point by the optical probe. (b) Frequency spectrum of the optically measured displacement from 0 to 18 MHz. (c) Expanded view of the S_1 ZGV mode resonances and thickness mode resonance.

$=0.525$ mm), peaks around 8 and 15 MHz can be ascribed to the ZGV resonance of S_1 and A_2 modes, respectively. Since the spectrum of the incident laser pulse is limited to 18 MHz, the excitation of the A_2 mode is less efficient than that of the S_1 mode. An expanded view of the frequency spectrum in the vicinity of the S_1 mode is shown in Fig. 2(c). The central part is composed of three sharp peaks. The quality factor $Q=2500$, deduced from the relative bandwidth ($Q=f/\Delta f$), is limited by the acquisition time. The peak at 8.03 MHz corresponds to the thickness resonance at the S_1 mode cut-off frequency $f_c=V_L/2d$, with $V_L=8433$ m/s and $d=0.525$ mm. In previous experiments on metallic plates,[11] the thickness mode resonance was not observed. Since silicon is partially transparent to near infrared radiation, the absorption of the YAG laser energy below the plate surface favors the generation of longitudinal waves and thus the excitation of the thickness extensional vibration. The amplitude modulation of the acoustic signal results from the beating of the S_1 thickness and ZGV modes. From the theoretical values of the minimum frequencies,

$$f_{0[100]}d = 4.044 \text{ MHz mm},$$

$$f_{0[110]}d = 4.069 \text{ MHz mm}, \quad (4)$$

for the [100] and [110] propagation directions, respectively, it appears that the other two peaks at 7.71 and 7.75 MHz correspond to the ZGV resonances for the S_1 mode in these directions. The laser source thus seems to preferentially excite local resonance for Lamb modes propagating in these directions. In order to confirm this hypothesis, the authors conducted another experiment where the point laser source used for Lamb wave excitation was replaced with a narrow line source.

A beam expander ($\times 7.5$) and a cylindrical lens (focal length 200 mm) were used to enlarge the laser beam and focus it to a narrow line on the plate surface. The optical energy distribution was close to a Gaussian and the absorbed power density was below the ablation threshold. The full length of the source at $1/e$ of the maximum value was found to be 12 mm and the width was estimated to be 0.3 mm. The plate was rotated from $\varphi=0°-360°$ in 1° steps and for each position the mechanical displacement was measured in the middle of the line. Figure 3(a) is a B-scan of the spectrum from 7.7 to 8.1 MHz. As expected, the thickness resonance frequency is independent of the line orientation. The ZGV resonance frequency, on the other hand, oscillates with a 90° period from the minimum value at $\varphi=0°$ to the maximum value at $\varphi=45°$. A 50-kHz frequency tuning can be achieved by rotating the line source.

The polar plot in Fig. 3(b) shows the amplitude of the ZGV resonance as a function of angle (φ) and maxima are observed at $\varphi=0°$ and 45° (and crystallographically equivalent directions). The authors assume that this effect could be explained by the deviation of the acoustic energy vector. In an anisotropic medium, the acoustic ray is normal to the slowness surface and, generally, is not collinear to the wave vector k. Figure 4 shows the slowness curve, i.e., the variations of the inverse of the S_1 ZGV phase velocity:

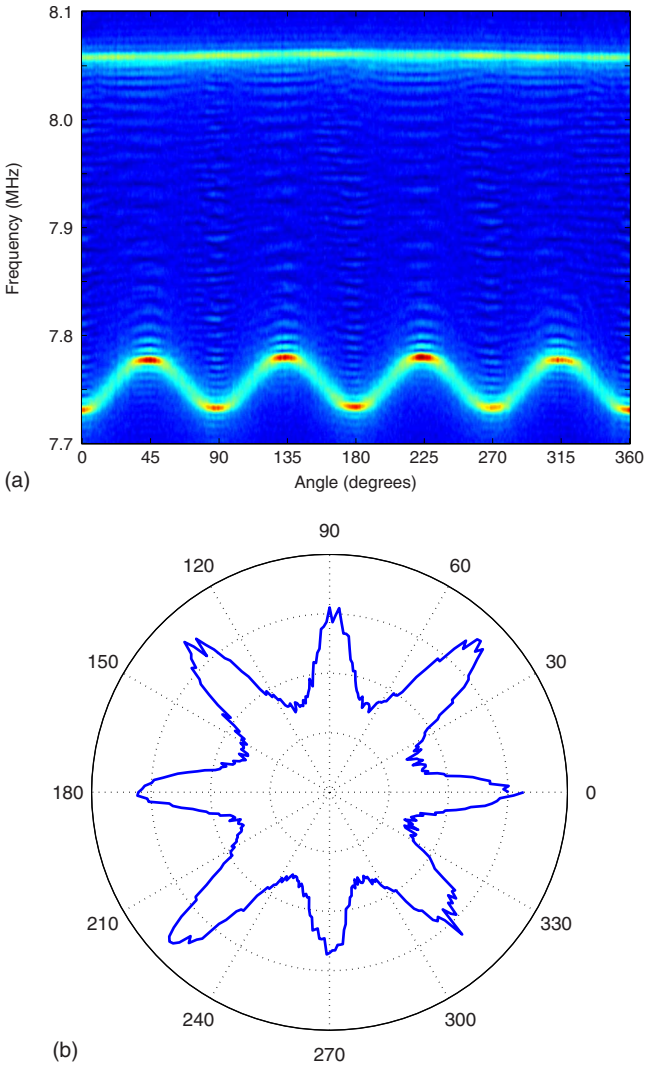

FIG. 3. (Color online) Line laser source. (a) *B*-scan of the spectrum measured as a function of the line orientation. The thickness resonance frequency is constant while the ZGV resonance frequency oscillates with a 90° period. (b) Polar plot (linear scale) of the resonance amplitude versus the propagation direction.

$$\frac{1}{V_0} = \frac{k_0}{2\pi f_0}, \tag{5}$$

plotted as a function of the propagation direction. The deviation of the energy velocity vector $\boldsymbol{V}_e$ from the wave vector

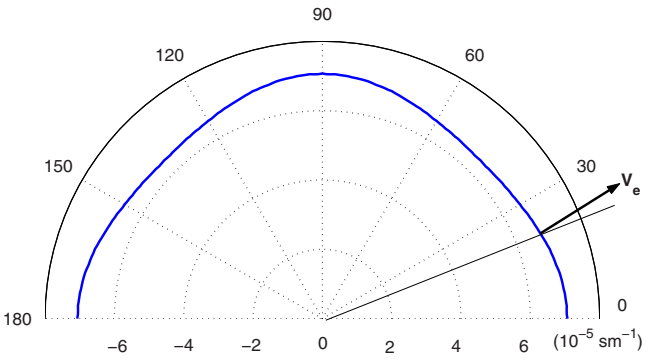

FIG. 4. (Color online) Slowness curve of the S_1 ZGV mode and deviation of the energy velocity vector $\boldsymbol{V}_e$.

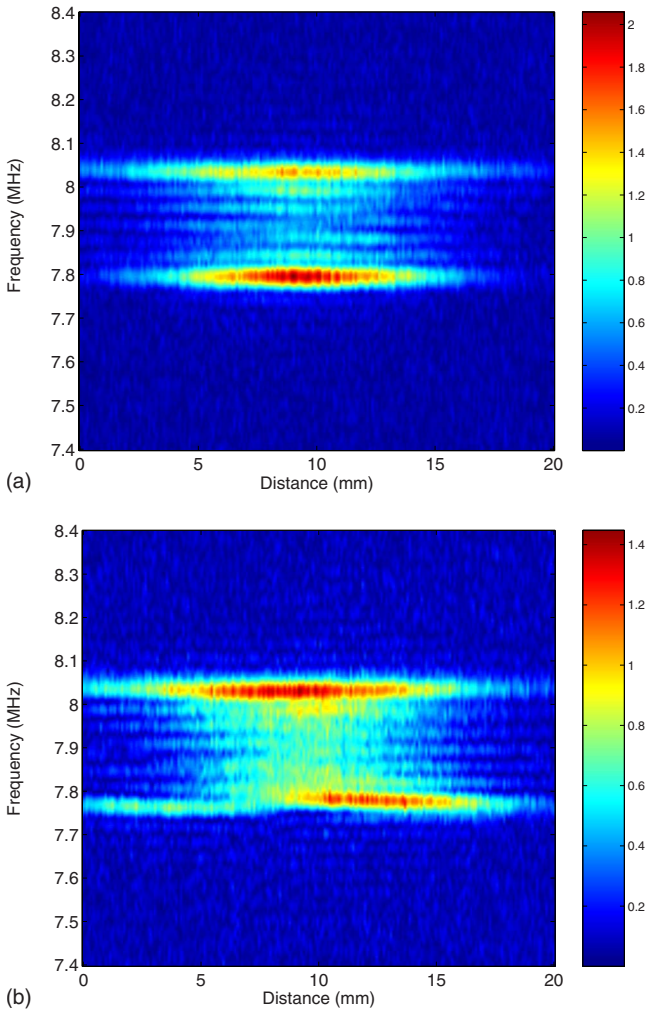

FIG. 5. (Color online) *B*-scan of the resonance amplitude measured along a line parallel to the source at a distance equal to 10 mm. (a) Line perpendicular to the direction $\varphi=0°$. (b) $\varphi=22.5°$: the energy distribution of the ZGV resonance is shifted from that of the thickness resonance mode.

vanishes for $\varphi=0°$ and 45° and reaches 10.1° for the direction $\varphi=22.5°$. In order to check that the acoustic beam is tilted, the amplitude of the resonances was measured along a line parallel to the source at a distance equal to 10 mm. Figure 5 is a frequency *B*-scan (± 10 mm apart from the center of the line source) in the [100] and in the intermediate ($\varphi=22.5°$) directions. As the thickness resonance is not sensitive to the plate anisotropy, the upper line in the plot is not deviated from the normal to the line source. Conversely, the lower line in Fig. 5(b) shows that the energy distribution of the ZGV resonance is shifted by 2.2 mm, corresponding to a beam deviation angle equal to about 12.4°, slightly higher than the expected value.

It was previously demonstrated that the ZGV resonance results from the interference of the two waves generated in opposite directions with comparable amplitudes by the line source.[19] Owing to the negative slope of the S_1 mode dispersion curve for $k<k_0$ (Fig. 1), these two counter-propagating modes have the same (small) group velocity. The standing wave pattern is oriented along the propagation direction of the acoustic energy. In an anisotropic plate and in noncrys-

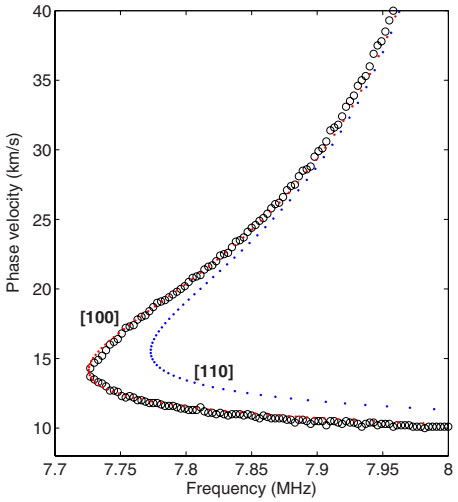

FIG. 6. (Color online) Phase velocity dispersion curves for a line source perpendicular to the [100] direction. Experimental points (circles) are compared with the theoretical curves computed for the S_1 Lamb mode propagating along [100]- and [110]-directions.

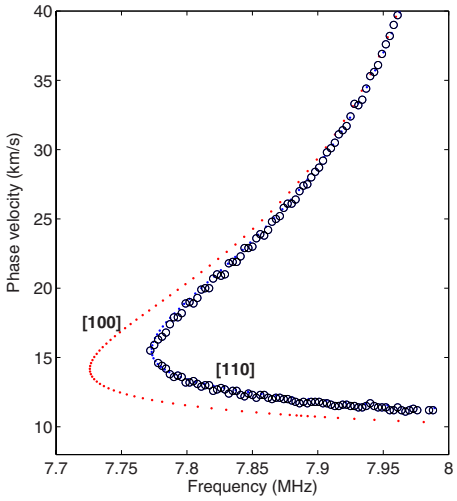

FIG. 7. (Color online) Phase velocity dispersion curves for a line source perpendicular to the [110] direction. Experimental points (circles) are compared with the theoretical curves computed for the S_1 Lamb mode propagating along [100]- and [110]-directions.

tallographic directions, the authors expected that the beam deviation reduces the efficiency of the interference and thus the amplitude of the ZGV resonance.

In order to identify the ZGV modes, they have measured the dispersion curves. For a given orientation of the line laser source, the distance r of the optical probe beam was varied from 0 to 12 mm in 0.1 mm steps. At each source to receiver distance, the normal displacement $u(r,t)$ was recorded during 100 μs with a 100 MHz sampling frequency. The measured signals are time Fourier transformed into $U(r,f)$. At each frequency, a spatial Fourier transform provides the spectrum in the time and spatial frequency domain:

$$\bar{U}(k,f) = \int U(r,f)e^{ikr}dr. \tag{6}$$

The spatial frequencies of the acoustic modes were determined by identifying the peaks in the power spectrum. Applying this procedure from 7.7 to 8 MHz allows us to plot the dispersion curves for the S_1 Lamb mode. The phase velocity dispersion curves for [100] and [110] propagation directions are shown in Figs. 6 and 7, respectively. Taken into account the small frequency range (300 kHz), experimental points are very close to the theoretical curves calculated for a plate thickness $d=0.5235$ mm. The maximum difference between theory and experiments (10 kHz) is on the order of the frequency resolution. As expected, the dispersion curves measured for other directions ($\varphi=22.5°$, for example) lie in between the curves calculated for [100]- and [110]-axis (Fig. 8).

The same signal processing was applied to the experimental data for frequencies around 15 MHz. Figure 9 shows that the high frequency peak in Fig. 2(b) can be ascribed to the minimum frequency of the A_2 Lamb mode. Due to the small signal to noise ratio, only the Fourier components close to the minimum frequency can be extracted from the experimental data. Nevertheless this ZGV mode is of great interest for the determination of the plate material properties. Simulations giving the shift in the resonance frequency for a 1% relative change of the elastic constants indicate that the S_1 ZGV Lamb mode is not sensitive to the variations of c_{12}. Conversely, the A_2 ZGV mode is very sensitive to the variations of c_{44} and relatively sensitive to a c_{12} change. The elastic constant c_{11} can be deduced directly from the thickness resonance frequency. Assuming a 15 kHz resolution in the frequency measurement, it is possible to determine c_{44} and c_{12} with 0.1% and 0.5% uncertainties, respectively, from the phase velocity dispersion curves in the minimum frequency region. The inversion of the dispersion data for a complete determination of the silicon elastic moduli is beyond the scope of this paper and may be accomplished following the approaches proposed in the literature.[20,21]

IV. CONCLUSION

The authors analyzed the mechanical response of a silicon plate to an excitation by a laser pulse focussed into a circular or a line source. The displacement normal to the

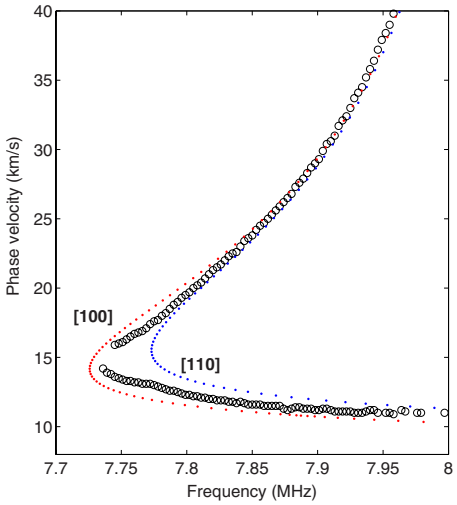

FIG. 8. (Color online) For a line source perpendicular to the 22.5° direction, experimental data (circles) lie in between the curves computed for the S_1 Lamb mode propagating along [100]- and [110]-directions.

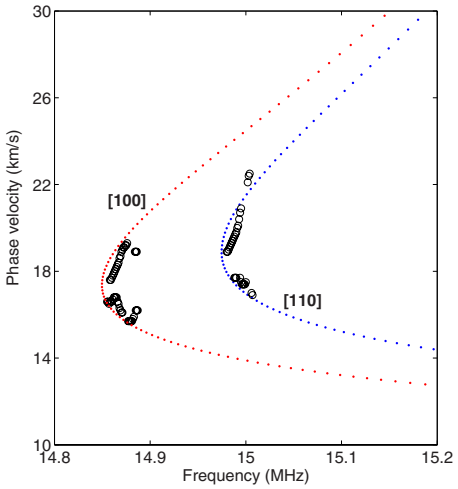

FIG. 9. (Color online) Phase velocity dispersion curves for a line source perpendicular to [100]- and [110]-directions. The experimental points (circles) are compared with the theoretical curves computed for the A_2 Lamb mode propagating along [100]- and [110]-directions.

plate surface was measured close to the source by a sensitive interferometer. This noncontact setup allows us to recover sharp peaks corresponding to the resonance of both thickness mode and ZGV Lamb modes. In contrast to the thickness resonance, ZGV resonances at the minimum frequency of Lamb mode dispersion curves are sensitive to the anisotropy of the plate material. Their amplitude and frequency depend on the orientation of the laser line source. In nonsymmetry directions and for a finite line source, the standing wave pattern resulting from the interference of the two counterpropagating waves is tilted from the normal to the line source. For the S_1 and A_2 ZGV Lamb modes, the minimum frequency is clearly identified from the comparison between experimental and theoretical dispersion curves. With an appropriate inversion algorithm, it should be possible to determine from these measurements the three elastic constants of the plate material with excellent accuracy.

[1]C. B. Scruby and L. E. Drain, *Laser Ultrasonics, Techniques and Applications* (Adam Hilger, New York, 1990).
[2]S. J. Davies, C. Edwards, G. S. Taylor, and S. B. Palmer, "Laser-generated ultrasound: Its properties, mechanisms and multifarious applications," J. Phys. D **26**, 329–348 (1993).
[3]L. F. Bresse, D. A. Hutchins, and K. Lundgren, "Elastic constant determination using generation by pulsed lasers," J. Acoust. Soc. Am. **84**, 1751–1757 (1988).
[4]S. E. Bobbin, J. W. Wagner, and R. C. Cammarata, "Determination of the flexural of thin films from measurements of the first arrival of the symmetric Lamb wave," Appl. Phys. Lett. **59**, 1544–1546 (1991).
[5]W. Gao, C. Glorieux, and J. Thoen, "Laser ultrasonic study of Lamb waves: Determination of the thickness and velocities of a thin plate," Int. J. Eng. Sci. **41**, 219–228 (2003).
[6]D. A. Hutchins, K. Lundgren, and S. B. Palmer, "A laser study of transient Lamb waves in thin materials," J. Acoust. Soc. Am. **85**, 1441–1448 (1989).
[7]J. A. Rogers and K. A. Nelson, "Study of Lamb acoustic waveguide modes in unsupported polyimide thin films using real-time impulsive stimulated thermal scattering," J. Appl. Phys. **75**, 1534–1556 (1994).
[8]J. A. Rogers, A. A. Maznev, M. J. Banet, and K. A. Nelson, "Optical generation and characterization of acoustic waves in thin films: Fundamentals and applications," Annu. Rev. Mater. Sci. **30**, 117–157 (2000).
[9]K. Yamanaka, Y. Nagata, and T. Koda, "Selective excitation of single-mode acoustic waves by phase velocity scanning of a laser beam," Appl. Phys. Lett. **58**, 1591–1593 (1991).
[10]C. Prada, O. Balogun, and T. W. Murray, "Laser-based ultrasonic generation and detection of zero-group velocity Lamb waves in thin plates," Appl. Phys. Lett. **87**, 194109 (2005).
[11]D. Clorennec, C. Prada, D. Royer, and T. W. Murray, "Laser impulse generation and interferometer detection of zero-group velocity Lamb modes," Appl. Phys. Lett. **89**, 024101 (2006).
[12]D. Clorennec, C. Prada, and D. Royer, "Local and noncontact measurement of bulk acoustic wave velocities in thin isotropic plates and shells using zero-group velocity Lamb modes," J. Appl. Phys. **101**, 034908 (2007).
[13]S. D. Holland and D. E. Chimenti, "High contrast air-coupled acoustic imaging with zero group velocity Lamb modes," Appl. Phys. Lett. **83**, 2704–2706 (2003).
[14]A. Gibson and J. S. Popovics, "Lamb wave basis for impact-echo method analysis," J. Eng. Mech. **131**, 438–443 (2005).
[15]B. Audoin, C. Bescond, and M. Deschamps, "Measurement of stiffness coefficients of anisotropic materials from pointlike generation and detection of acoustic waves," J. Appl. Phys. **80**, 3760–3771 (1996).
[16]D. Royer and E. Dieulesaint, *Elastic Waves in Solids* (Springer, Berlin, 1999), Vol. **1**.
[17]B. Pavlakovic and M. Lowe, DISPERSE software, v.2.0.16. Mechanical Engineering, Imperial College, London, 2005.
[18]D. Royer and E. Dieulesaint, in *Proceedings of the 1986 IEEE Ultrasonics Symposium* (IEEE, New York, 1986), p. 527.
[19]C. Prada, D. Clorennec, and D. Royer, "Local vibration of an elastic plate and zero-group velocity Lamb modes," J. Acoust. Soc. Am. **124**, 203–212 (2008).
[20]M. R. Karim, A. K. Mal, and Y. Bar-Cohen, "Inversion of leaky Lamb wave data by simplex algorithm," J. Acoust. Soc. Am. **88**, 482–491 (1990).
[21]S. I. Rokhlin and D. E. Chimenti, "Reconstruction of elastic constants from ultrasonic reflectivity data in a fluid coupled composite plate," Rev. Prog. Quant. Nondestr. Eval. **9B**, 1411–1418 (1990).